

Synthesis and Thermal Decomposition of a Polymeric Precursor of the $\text{La}_2\text{Mo}_2\text{O}_9$ Compound

R. A. Rocha and E. N. S. Muccillo*

Centro Multidisciplinar para o Desenvolvimento de Materiais Cerâmicos, CCTM-Instituto de Pesquisas Energéticas e Nucleares, Av. Prof. Lineu Prestes, 2242, Cidade Universitária, S. Paulo, 05508-000, SP, Brazil

Received May 28, 2003

A polymeric precursor of the phase $\text{La}_2\text{Mo}_2\text{O}_9$ was prepared by the in situ polymerizable complex method. For comparison purposes polymeric precursors of the La and Mo cations were also independently prepared and characterized. Thermal analysis results show that the polymer precursor of $\text{La}_2\text{Mo}_2\text{O}_9$ has a crystallization temperature near 550 °C and characteristic decomposition behavior when compared to the decomposition of the individual cation polymeric precursors. Fourier transform infrared spectroscopy results corroborate this observation. Scanning electron microscopy micrographs reveal a different morphology of powder particles after calcining at selected temperatures. Powder X-ray diffraction patterns were obtained for phase identification.

Introduction

The lanthanum molybdate compounds have been investigated over the last 30 years. The equilibrium diagram of this system presents a number of phases with different physical properties.¹ These properties are recognized as a consequence of their crystal structure and of the Mo oxidation states. It was recently found that the high-temperature phase of the $\text{La}_2\text{Mo}_2\text{O}_9$ composition has interesting electrical properties and was proposed as a potential candidate for applications as a solid electrolyte.² At temperatures lower than 580 °C the low-symmetry α - $\text{La}_2\text{Mo}_2\text{O}_9$ phase is stable. The ionic conductivity of this α -phase is almost 2 orders of magnitude lower than that of the high-temperature β -phase. At temperatures higher than ~580 °C, the cubic β - $\text{La}_2\text{Mo}_2\text{O}_9$ is formed. It was shown³ that this phase presents a value of ionic conductivity similar to that of yttria-stabilized zirconia. It was also shown that the high-temperature β -phase can be obtained at lower temperatures by means of suitable substitutions with a number of cations and anions.^{2–6} In most of these studies, the lanthanum molybdate compounds were synthesized by solid-state reactions.^{1–6} Other techniques of synthesis used to prepare the $\text{La}_2\text{Mo}_2\text{O}_9$ composition were high-energy milling⁷ and a modified sol–gel⁸ process.

It is generally known that the synthesis of ceramic compounds by wet-chemical methods are preferred to those methods employing reactions in the solid state because they may give rise to more homogeneous powders with controlled stoichiometry.⁹

In this work, the technique of synthesis known as in situ polymerizable complex or polymeric precursor method¹⁰ was used for the preparation of the $\text{La}_2\text{Mo}_2\text{O}_9$ phase. This technique is based on the chelation of metal cations with a hydroxycarboxylic acid and in further polyesterification with a polyhydroxy alcohol. It was originally proposed for the preparation of coatings and capacitors,¹¹ and several ceramic materials with high chemical homogeneity and controlled stoichiometry were prepared by this technique so far, including those phases that are not in thermodynamic equilibrium or phases containing transition metal oxides.^{12,13} In this work we present a systematic study on the synthesis and thermal decomposition of the polymeric precursor of the $\text{La}_2\text{Mo}_2\text{O}_9$ compound. Results of thermal analyses will be compared to those of infrared spectroscopy to obtain further insight into the molecular constitution of precursors used in this technique. This study was also undertaken to establish an alternative procedure for the preparation of this ceramic material.

Experimental Section

* To whom correspondence should be addressed. E-mail: enavarro@ipen.br.

(1) Fournier, J. P.; Fournier, J.; Kohlmuller, R. *Bull. Soc. Chim. Fr.* **1970**, 12, 4277.

(2) Lacorre, P.; Goutenoire, F.; Bohnke, O.; Retoux, R.; Laligant, Y. *Nature* **2000**, 404, 856.

(3) Goutenoire, F.; Isnard, O.; Suard, E.; Bohnke, O.; Laligant, Y.; Retoux, R.; Lacorre, P. *J. Mater. Chem.* **2001**, 11, 119.

(4) Wang, X. P.; Fang, Q. F. *J. Phys.: Condens. Matter* **2001**, 13, 1641.

(5) Arulraj, A.; Goutenoire, F.; Tabellout, M.; Bohnke, O.; Lacorre, P. *Chem. Mater.* **2000**, 14, 2492.

(6) Khadasheva, Z. S.; Venskovskii, N. U.; Safronenko, M. G.; Mosunov, A. V.; Politova, E. D.; Stefanovich, S. Yu. *Inorg. Mater.* **2002**, 38, 1168.

(7) Lacorre, P.; Retoux, R. *J. Sol. Stat. Chem.* **1997**, 132, 443.

La_2O_3 (99.9%, IPEN) and MoO_2 (99%, Alfa Aesar) were used as starting materials. The lanthanum oxide was synthesized at our Institute from a rich-cerium concentrate by the ion-exchange resin and the fractionated precipitation techniques. A

(8) Kuang, X.; Fan, Y.; Yao, K.; Chen, Y. *J. Solid State Chem.* **1998**, 140, 354.

(9) Johnson, D. W., Jr. *Am. Ceram. Soc. Bull.* **1981**, 60, 221.

(10) Kakihana, M. *J. Sol-Gel Sci. Technol.* **1996**, 6, 7.

(11) Pechini, M. P. U.S. Patent 3,330,697, July 1967.

(12) Tai, L.-W.; Lessing, P. A. *J. Mater. Res.* **1992**, 7, 511.

(13) Zanetti, S. M.; Leite, E. R.; Longo, E.; Varela, J. A. *J. Mater. Res.* **1998**, 13, 2932.

lanthanum nitrate solution was prepared by dissolution of the La_2O_3 in a hot nitric acid solution. The molybdenum nitrate solution was prepared in a similar way as that of lanthanum nitrate, except by the addition of a suitable amount of hydrogen peroxide to promote the oxidation of molybdenum. A mixed nitrate solution was then prepared by mixing the individual nitrate solutions in the stoichiometric proportion under vigorous stirring. Other reagents such as nitric acid (65%, PA), anhydrous citric acid (99.5%), and ethylene glycol (99%) were utilized for the preparation of powders by the polymeric precursor technique. A citric acid solution was added to the mixed nitrate solution under heating and stirring. The ethylene glycol was then added to this mixed citrate solution to promote the polymerization. With continued heating at ~ 80 °C over several hours, the solution became viscous, and finally it gelled, forming a polyester-type resin. The main advantages attributed to this synthesis technique are the control of stoichiometry and a random distribution of cations in the polymeric chain, thereby ensuring chemical and microstructural homogeneities in the powder material.⁹ In the synthesis of the composition $\text{La}_2\text{Mo}_2\text{O}_9$ (229 composition), a metal:citric acid 1:2 molar ratio and a citric acid:ethylene glycol of 60:40 mass ratio were used. The polymeric precursor of lanthanum is colorless. In contrast, the color of the molybdenum precursor and that of the 229 composition changed from light yellow to dark blue during the polymerization reaction due to the change of the molybdenum valence.¹⁴ The polymeric precursors were dried at 45 °C before characterization. After the pyrolysis at 200 °C followed by calcination at 550 or 700 °C for 3 h, white powders were obtained.

The thermal decomposition of a polymer sample without any cation, hereafter called bare sample, the individual cation polymers, and the 229 composition polymeric precursors were characterized by simultaneous thermogravimetry, TG, and differential thermal analysis, DTA (STA 409, Netzsch), from room temperature up to 700 °C. In all experiments, α -alumina (Alumalux, Alcoa) was used as reference material. The heating and cooling rates were 3 and 5 °C min⁻¹, respectively, in a dynamic atmosphere of synthetic air ($\sim 20\%$ O₂).

The precursor materials, the individual cation polymers, and the 229 composition before and after calcination at different temperatures were characterized by Fourier transform infrared spectroscopy, FTIR (Magna IR 560, Nicolet), in the 400–4000-cm⁻¹ range. The precursors were mixed to KBr for this analysis.

After calcination at selected temperatures the morphology of the 229 composition powder materials was observed by scanning electron microscopy, SEM (XL 30, Philips), using secondary electrons.

The amorphous and crystalline structures were determined by the powder X-ray diffraction, XRD, method using a diffractometer (D8 Advance, Bruker-AXS) equipped with a Ni-filtered Cu K α radiation source. The operating conditions were 40 kV and 40 mA. Scans were conducted at a sampling interval of 0.05° and counting time of 10 s in the 15–75° 2 θ range.

Results and Discussion

Figure 1 shows TG and DTA curves of the bare sample. The weight loss occurs continuously from 200 to 500 °C. In this temperature range the total weight loss was 99.2%. The residual material may be attributed to impurities present in the starting chemicals, assuming that the polymeric precursor is decomposed at such a high temperature. The DTA curve exhibits endothermic peaks at 70 and 240 °C. The first endothermic peak is assigned to a dehydration reaction and the second to the polyester fusion, in agreement with the tempera-

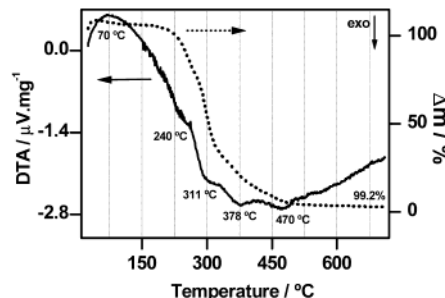


Figure 1. TG/DTA curves of the bare sample.

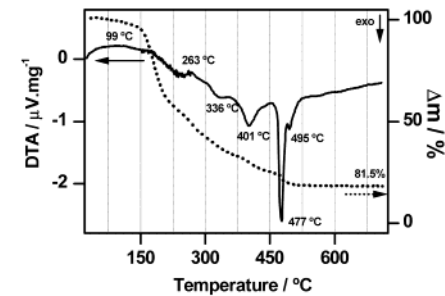


Figure 2. TG/DTA curves of the Mo polymeric precursor.

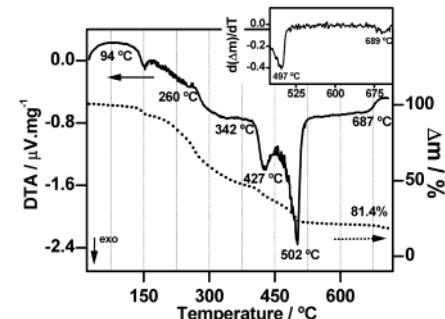


Figure 3. TG/DTA curves of the La polymeric precursor.

tures at which these phenomena occur.¹⁵ The exothermic peaks may be attributed to the burnout of organic material. Thus, exothermic peaks should be related to the polyester decomposition (311 °C), to the combustion of organic matter (378 °C), and to decomposition of the combustion products (470 °C). This result agrees with a previous study¹² on the decomposition of this type of resin for which the burnout of most organic substances occurs up to approximately 500 °C.

The results of thermal analyses of the molybdenum polymer are shown in Figure 2. The total weight loss was 81.5% and it occurred in two steps up to 500 °C. The DTA curve reveals endothermic and exothermic peaks in temperature ranges similar to those occurring for the bare sample. In the second step of weight loss (450–500 °C), two exothermic peaks are observed. The first exothermic peak at 477 °C is very sharp and may be attributed to the crystallization of molybdenum oxide, whereas the peak at 495 °C may be related to an oxidation reaction of the molybdenum oxide.

The TG and DTA curves of the lanthanum polymer are shown in Figure 3. The total weight loss was 81.4% and it occurred up to 700 °C. However, most of the weight was lost up to 500 °C. The DTA curve shows

(14) Killeffer, D. H.; Linz, A. *Molybdenum Compounds—Their Chemistry and Technology*; Interscience Publishers: New York, 1952.

(15) Kroschitz, J. I., Ed. *Concise Encyclopedia of Polymer Science and Engineering*; John Wiley & Sons: New York, 1990.

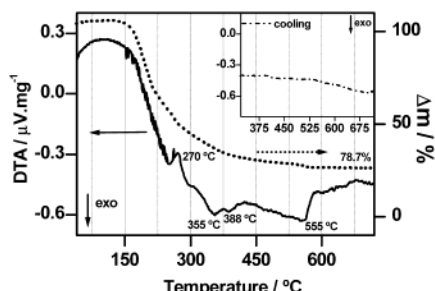


Figure 4. TG/DTA curves of the polymeric precursor of the 229 composition.

endothermic and exothermic events similar to those of the bare sample. The exothermic peak at approximately 687 °C is attributed to the decomposition of an intermediate lanthanum compound. The insert in this figure shows the high-temperature part of the derivative of the TG curve, DTG. A peak at 689 °C is clearly seen in this curve. The weight loss associated with this peak may be attributed to the decomposition of a lanthanum oxycarbonate, $\text{La}_2\text{O}_2\text{CO}_3$, which is known to be readily formed as a result of the reaction between an intermediate product of the lanthanum nitrate decomposition and CO_2 from the atmosphere.¹⁶

Figure 4 shows TG and DTA curves of the 229 composition polymer. The total weight loss was 78.7% and most of it occurred between 150 and 400 °C. The DTA curve presents endothermic and exothermic peaks similar to those observed for other polymeric precursors. The broad exothermic peak at 555 °C comprises two peaks assigned to the decomposition of combustion products and the crystallization of the $\text{La}_2\text{Mo}_2\text{O}_9$ phase. The insert in this figure shows the DTA curve during the cooling cycle. This curve does not present any thermal event that could be assigned to a phase transition.

These results show that the thermal events detected in the polymeric precursors are the same as those in the bare sample. The observed shifts in the temperature of similar thermal events are due to differences in the strength of the interaction between metallic cations and the polymer.

Recent studies^{16,17} on the decomposition of the lanthanum nitrate in air have shown that the nitrate precursor decomposes, forming an oxynitrate (LaONO_3), which reacts with CO_2 from the atmosphere, resulting in an oxycarbonate of lanthanum ($\text{La}_2\text{O}_2\text{CO}_3$). This reaction occurs in the 410–470 °C temperature range. This oxycarbonate has a low-symmetry crystal structure and transforms to a hexagonal structure at 480 °C. The total decomposition of the $\text{La}_2\text{O}_2\text{CO}_3$ occurs only for temperatures higher than 650 °C. The formation of an oxycarbonate compound in the decomposition of the lanthanum polymer shows that the same decomposition path should occur in the lanthanum nitrate and in the lanthanum polymeric precursor. In this case, the main expected difference in the decomposition reaction should be related to the temperature at which it occurs.

It is worth noting that this oxycarbonate compound was not observed to be formed in the decomposition of

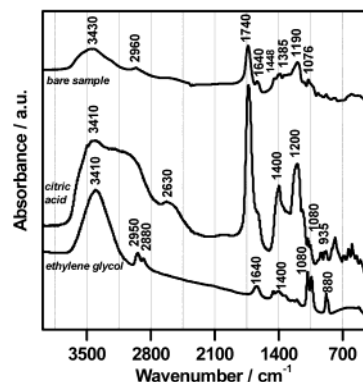


Figure 5. FTIR spectra of the precursor chemicals and the bare sample.

the 229 composition polymer. Therefore, these results suggest that, in the 229 polymeric precursor, the La and Mo cations are not chelated as individual cations but as a compound with a specific decomposition behavior and characteristic crystallization temperature.

To obtain better insight into the structure and composition of the precursor materials, FTIR spectra were obtained for chemical precursors, the bare sample, the individual cation polymers, the 229 composition polymer, and after pyrolysis of these precursors at selected temperatures.

Figure 5 shows FTIR spectra for the precursor chemicals and for the bare sample. Spectra of citric acid and ethylene glycol correlate with literature data.^{18,19} In the spectrum of the bare sample a broad band at $\sim 3430 \text{ cm}^{-1}$ related to a single bridge OH vibration can be seen. Other vibrations are as follows: CH_2 stretching ($\sim 2960 \text{ cm}^{-1}$), CH_2 deformation ($\sim 1448 \text{ cm}^{-1}$), O–H deformation or C–O stretching ($\sim 1385 \text{ cm}^{-1}$), C–O stretching ($\sim 1190 \text{ cm}^{-1}$), and symmetric ($\sim 1076 \text{ cm}^{-1}$) and asymmetric ($\sim 1040 \text{ cm}^{-1}$) C–O stretching. The strong vibration at 1740 cm^{-1} is related to the C=O stretching mode for ester groups (R–COO–R). These groups are formed during the polyesterification reaction. A small vibration at 1640 cm^{-1} is due to COO^- stretching. It may also indicate the presence of a chelated ester, once the starting chemicals are not free of impurities.

The FTIR spectra of individual cation polymers and those of La and Mo polymeric precursors calcined at 700 and 550 °C, respectively, are shown in Figure 6. Spectra of dried La and Mo polymers show infrared bands similar to those observed in the bare sample spectrum. In the spectrum of the La polymer (Figure 6a) other vibrations are due to the following: H_2O ($\sim 3477 \text{ cm}^{-1}$), OH stretching ($\sim 3415 \text{ cm}^{-1}$), C=O stretching mode of the ester ($\sim 1734 \text{ cm}^{-1}$), COO^- vibration of a chelated ester ($\sim 1637 \text{ cm}^{-1}$), CH_2 or OH deformation ($\sim 1400 \text{ cm}^{-1}$), NO_3^- vibration ($\sim 1385 \text{ cm}^{-1}$), and C–O stretching or OH deformation ($\sim 1220 \text{ cm}^{-1}$). The presence of bands characteristics of nitrate ions (~ 1385 and $\sim 840 \text{ cm}^{-1}$) should be noted. These nitrate bands are probably related to the oxynitrate formed during storage of the polymer at 45 °C. This result agrees with that of thermal analysis results (Figure 3). For the La poly-

(16) Gobichon, A. E.; Auffrédic, J. P.; Loüer, D. *Solid State Ionics* **1997**, 93, 51.

(17) Klingenberg, B.; Vannice, M. A. *Chem. Mater.* **1996**, 8, 2755.

(18) Bellamy, L. J. *The Infrared Spectra of Complex Molecules*; Methuen & Co.: London, 1954.

(19) Szymanski, H. A. *Interpreted Infrared Spectra Vol. 2*; Plenum Press: New York, 1966.

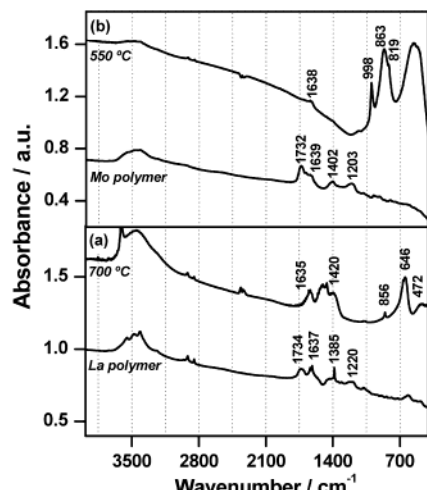


Figure 6. FTIR spectra of the La and Mo polymeric precursors before and after calcination.

meric precursor pyrolyzed at 200 °C and calcined at 700 °C, these nitrate-related vibrations are no longer observed. However, new vibrations at ~ 1420 and 856 cm^{-1} , which are characteristic of CO_3^{2-} carbonate groups, are clearly seen. In addition, an intense vibration at 646 cm^{-1} and a medium intensity vibration at 472 cm^{-1} are observed. These vibrations at wavenumbers lower than $\sim 700\text{ cm}^{-1}$ are usually associated with a metal–oxygen bond and, in this case, they may occur due to a partial decomposition of the La oxycarbonate at temperatures higher than 650 °C. These FTIR results are in general agreement with those of thermal analysis and demonstrate that the thermal decomposition of the lanthanum polymeric precursor occurs according to the same chemical reactions as those for the lanthanum nitrate.

The FTIR spectrum of the Mo polymeric precursor (Figure 6b) has the main vibrations assigned to H_2O ($\sim 3430\text{ cm}^{-1}$), OH stretching ($\sim 3420\text{ cm}^{-1}$), C=O stretching mode of the ester ($\sim 1732\text{ cm}^{-1}$), COO^- vibration of the chelated ester ($\sim 1638\text{ cm}^{-1}$), CH_2 or OH deformation ($\sim 1402\text{ cm}^{-1}$), and C–O stretching ($\sim 1203\text{ cm}^{-1}$). In this case, any vibrations associated with nitrate ions have not been detected.

It is worth noting the absorption bands attributed to free citric acid in the Mo ($\sim 3548\text{ cm}^{-1}$) and La ($\sim 3554\text{ cm}^{-1}$) polymers spectra. This infrared band appears as a consequence of the excess citric acid used in the synthesis to ensure the complexation of all cations in the starting solution.

Another important feature in these spectra, when compared to that of the bare sample, is the intensity ratio of bands at $\sim 1740\text{ cm}^{-1}$ and $\sim 1640\text{ cm}^{-1}$. The increase in the intensity of the 1640-cm^{-1} band relative to that of the 1740 cm^{-1} band is attributed to the existence of a chemical bond between metallic cations and the polymer chain.

The FTIR spectrum of a Mo polymeric precursor after pyrolysis at 200 °C and calcination at 550 °C exhibits vibrations due to chelated ester ($\sim 1638\text{ cm}^{-1}$) and intense vibrations at ~ 998 , ~ 863 , and $\sim 819\text{ cm}^{-1}$ assigned to the metal–oxygen bond of the MoO_3 ,²⁰

(20) Du, X.; Dong, L.; Li, C.; Liang, Y.; Chen, Y. *Langmuir* **1999**, 15, 5, 1693.

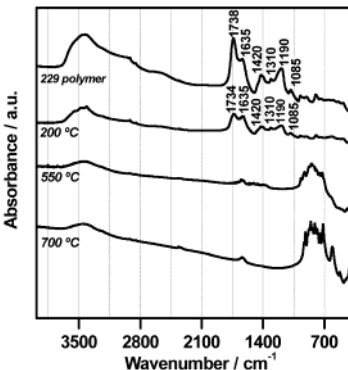


Figure 7. FTIR spectra of the 229 composition polymeric precursor before and after pyrolysis and calcination.

besides a broad absorption band in the $450\text{--}600\text{-cm}^{-1}$ interval, which could not be identified as a vibration of $\text{Mo(IV)}\text{--O}$ or $\text{Mo(VI)}\text{--O}$ bonds.

Figure 7 shows FTIR spectra of the 229 composition polymer before and after pyrolysis at 200 and further calcination at 550 and 700 °C. For the 229 polymer, the main infrared bands are related to the following: H_2O ($\sim 3430\text{ cm}^{-1}$), C=O stretching mode of the ester ($\sim 1738\text{ cm}^{-1}$), COO^- vibration of the chelated ester ($\sim 1635\text{ cm}^{-1}$), COO^- stretching (~ 1420 and $\sim 1310\text{ cm}^{-1}$), C–O stretching ($\sim 1190\text{ cm}^{-1}$), and symmetric C–O stretching ($\sim 1085\text{ cm}^{-1}$). In this spectrum the existence of free citric acid cannot be verified because the corresponding infrared band may overlap with that of H_2O . In addition, vibrations associated with carbonate or nitrate groups are not observed in this spectrum. All these considerations are in general agreement with thermal analysis results. An important observation that should be pointed out is that the FTIR spectrum of the 229 polymeric precursor cannot be interpreted in terms of a simple superposition of the individual La polymer and Mo polymer FTIR spectra. This should, in turn, indicate that La and Mo cations have a strong interaction during chelation. A similar observation has been done in the study of BaTiO_3 ceramic powder prepared by this technique.²¹

It can be generally observed that after any heat treatment there is a decrease in the intensity of those bands associated with carbon bonds. In the spectrum of the specimen pyrolyzed at 200 °C, most of the infrared bands found in the dried polymeric precursor are observed, indicating that the polymer did not decompose at this temperature. Calcination of the 229 composition polymer at higher temperatures (550 or 700 °C) produces the disappearance of the band due to C=O stretching of the ester ($\sim 1740\text{ cm}^{-1}$). However, the band assigned to the bond of the metal cations in the polymeric chain (chelated ester) at $\sim 1640\text{ cm}^{-1}$ is still observed. The detection of new absorption bands in the wavenumber range characteristic of metallic cations–oxygen bonds should be noted.

The morphologies of powder particles of the 229 polymeric precursor calcined at 550 and 700 °C are shown in parts a and b, respectively, of Figure 8. These micrographs evidence the degree of agglomeration of

(21) Kakihana, M.; Yoshimura, M. *Bull. Chem. Soc. Jpn.* **1999**, 72, 1427.

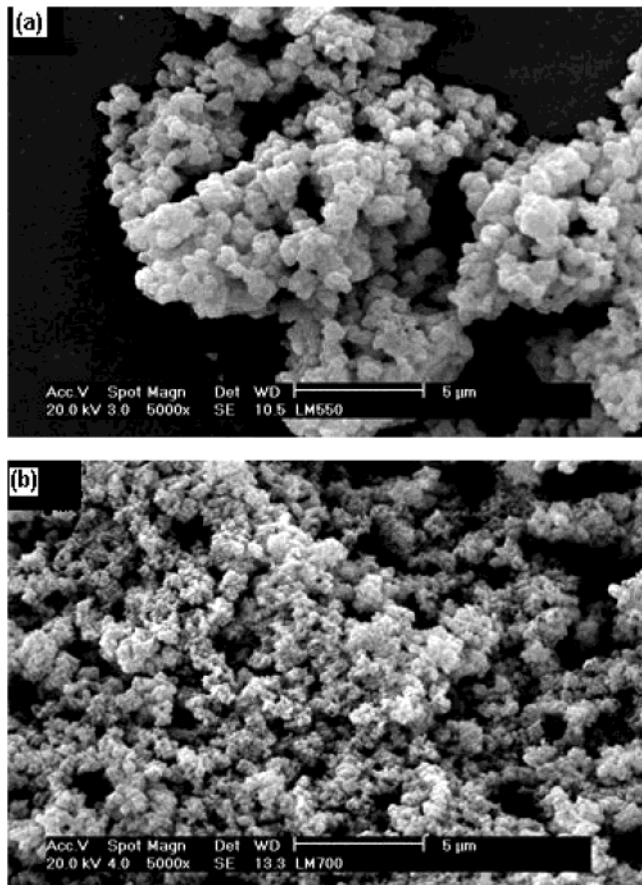


Figure 8. SEM micrographs of the 229 polymeric precursor after calcination at 550 °C (top) and 700 °C (bottom).

these powders. It should be noted that the agglomerated particles are approximately spherical in shape. Moreover, the sizes are in the nanometer range, although the powder calcined at lower temperature (550 °C) is apparently composed of particles with average size greater than that of the material calcined at a higher temperature (700 °C). This result may be caused by a crystallite size effect on the $\alpha \leftrightarrow \beta$ phase transition, as proposed earlier.⁸ However, the actual mechanism as to why this occurs is outside the scope of this paper.

Figure 9 shows X-ray diffraction patterns of the 229 composition polymer after pyrolysis at 200 °C and after further calcination at 500 or 700 °C. It can be seen in these XRD patterns that the pyrolyzed precursor con-

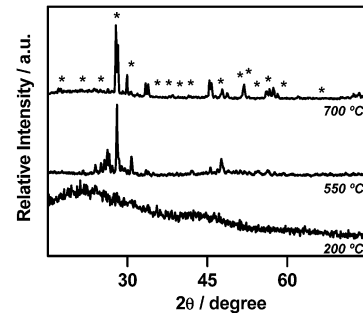


Figure 9. X-ray diffraction patterns of the 229 composition after pyrolysis (200 °C) and calcination at 500 or 700 °C. The symbol * refers to the β - $\text{La}_2\text{Mo}_2\text{O}_9$ phase.

sisted of amorphous material, while calcined powders were crystalline in nature. Most of the high-intensity XRD peaks correspond to those of the β - $\text{La}_2\text{Mo}_2\text{O}_9$ (space group $P2_13$). Moreover, the intensity of the noncubic phase reflections increased as the calcination temperature increased.

Conclusions

Ultrafine powders resulting from the thermal decomposition of a polymeric precursor of the $\text{La}_2\text{Mo}_2\text{O}_9$ composition were successfully prepared by the in situ polymerizable complex method. Results on thermal analyses support the theory that the La and Mo cations are chelated as a compound and not individually in the polymer network. The high-temperature cubic phase of $\text{La}_2\text{Mo}_2\text{O}_9$ could be directly obtained by calcination of the precursor material at relatively low temperatures. The in situ polymerizable complex method proved to be an alternative and suitable route for the preparation of lanthanum molybdate compounds.

Acknowledgment. Financial support from FAPESP (99/10798-0, 95/05172-4, 96/09604-9, 97/06152-2), CNPq (300934/94-7), Pronex, and CNEN are greatly acknowledged. R. A. Rocha acknowledges FAPESP (01/12269-7) for the scholarship.

CM030413+